Proceedings of the 9th U.S. National and 10th Canadian Conference on Earthquake Engineering
Compte Rendu de la 9ième Conférence Nationale Américaine et
10ième Conférence Canadienne de Génie Parasismique
July 25-29, 2010, Toronto, Ontario, Canada • Paper No 327

FINITE ELEMENT INVESTIGATION AND DESIGN RECOMMENDATIONS FOR PERFORATED STEEL PLATE SHEAR WALLS

Ronny Purba[1] and Michel Bruneau[2]

ABSTRACT

This paper presents results from an investigation of the behavior of unstiffened thin SPSW having a regular pattern of openings (a.k.a. perforated SPSW). Finite element monotonic pushover analyses were conducted, first on a series of individual perforated strips with variation in perforation diameter, to develop a fundamental understanding of the behavior of complete perforated SPSW, then on a corresponding series of complete perforated SPSW having various perforation diameters and three different set of wall boundary conditions. Though some differences between the SPSW panel strips and the individual strip results are observed at large monitored strain, at lower monitored strain however the two models are in a good agreement. Based on the analytical results design recommendations of these perforated SPSWs are presented.

Introduction

Steel plate shear walls (SPSW) have been rapidly gained interest in recent years as an effective lateral force resisting system. A key feature of SPSW systems is the significant stiffness and strength they can provide to buildings compared to other lateral force resisting systems. However, in some SPSW applications, the minimum available thickness of infill plate might be thicker such than required by design. Per capacity design principles, at development of the system's plastic mechanism, yielding of the SPSW infill plates will induce relatively large forces to the surrounding frames and consequently will increase the sizes of horizontal and vertical boundary members to which the infill plates are connected. A number of solutions have been proposed to alleviate this concern, either by changing properties of the infill plate via using thin light-gauge cold-rolled (Berman and Bruneau 2005), using low yield strength steel (Vian and Bruneau 2005), or introducing multiple regularly spaced perforations, also known as perforated SPSW (Vian and Bruneau 2005). The later solution is appealing as it can at the same time accommodate the need for utility systems to pass-through the infill plate, without detrimental effects to the SPSW.

[1]Graduate Research Assistant, Dept. of Civil, Structural and Environmental Engineering, University at Buffalo, Amherst, NY 14260. Email: rpurba@buffalo.edu
[2]Professor, Dept. of Civil, Structural and Environmental Engineering, University at Buffalo, Amherst, NY 14260. Email: bruneau@buffalo.edu

This paper presents the results of an investigation to better understand one aspect of the behavior of unstiffened thin perforated SPSW, more specifically the distribution of yielding around the regularly spaced openings on the infill plate and related requirements to achieve adequate ductile performance, as drift demands relate to infill plate elongations demands. Finite element (FE) monotonic pushover analysis of sub-element (strips) and full specimens are conducted. Based on the analytical results design recommendations and consideration of these perforated SPSW are presented.

Previous Research on Steel Plate Shear Walls

Much research has been conducted since the mid 1980's on SPSW, as summarized in Sabelli and Bruneau (2007). Early studies by Thorburn *et al.* (1983) introduced the relatively simple *Strip Model* to represent the behavior of unstiffened thin SPSW. This model has been demonstrated to generally provide good results (Timler and Kulak 1983; Driver 1997). More recently, some researchers have used FE to investigate issues related to SPSWs.

Driver *et al.* (1997) developed FE models to investigate a large scale, four-story, single bay unstiffened SPSW having moment-resisting beam-to-column connections and tested by quasi-static cyclic loading. Eight-node quadratic shell elements (S8R5) were used for infill plates directly connected to three-node quadratic beam element (B32) for the beams and columns. Initial imperfections of 10 mm based on the first buckling mode of the plate and residual stresses were also incorporated in the FE model. It was found that omitting geometric nonlinearity and second order effects in the FE model caused discrepancy between the cyclic experimental and the analytical results, as pinching of the hysteretic loops was not replicated. Behbahanifard *et al*. (2003) investigated a three story specimen created by removing the lower story of the four-story specimen tested by Driver *et al*. (1997). The specimen was tested under lateral quasi-static cyclic loading in the presence of gravity loads. A nonlinear FE model was developed using ABAQUS/Explicit v. 6.2 to accurately simulate the monotonic and cyclic behaviors of the test specimen. Four-node shell elements with reduced integration (S4R) were used for the entire SPSW. Material and geometric nonlinearity were considered in the FE model. However, residual stresses and plastic deformations from the previous test were not considered due to their complexity. Good agreement was obtained, although the analytical strength underestimated the experimental strength. Both the Driver *et al*. (1997) and the Behbahanifard *et al*. (2003) studies focused on SPSW with solid infill plates.

Vian and Bruneau (2005) conducted analytical and experimental work on SPSW with staggered holes of diameter 200 mm arranged at a 45° angle with 300 mm center-to-center spacing along both the vertical and horizontal directions on the infill plate. The perforated infill plate of 2.6 mm thick was made of Low Yield Steel (LYS) with yield stress of 165 MPa framed by 4000 mm x 2000 mm centerline dimensions with I-shaped sections W18X65 (beams) and W18X71 (columns), and Reduced Beam Sections (RBS) connections. In addition, Vian and Bruneau (2005) conducted FE analyses on simplified models to replicate the experimental results. These simplified analytical models were extended to consider various perforation diameters using steel typically specified in North American construction projects. Results illustrated general trends but some erratic jaggedness in the results. The researchers called for further parametric studies to investigate the causes of the observed variability.

This paper undertakes such an investigation, comparing results obtained from individual perforated strip models and full SPSW in terms of structural behavior as well for monitored maximum strain as a function of total strip elongation.

Finite Element Analysis of Individual Perforated Strip

FE models of individual perforated strips were developed to provide an understanding of their behavior as a fundamental building block in understanding the behavior of complete perforated SPSW. The commercially available software ABAQUS/Standard v. 6.5-1 was used for all analyses in this study. Typical perforated strips of length L equal to 2000 mm, diagonal width S_{diag} equal to 400 mm, perforation diameter D ranging from 10 to 300 mm, number of perforations along the diagonal strip N_r equal to 4, and plate thickness t_p equal to 5 mm were investigated (Fig. 1a). Because the strip geometry and loading are symmetrical about horizontal and vertical axes through the center of the strip, a quadrant of the full-strip is modeled with proper constraints along the symmetric boundaries (Fig. 1b).

A monotonic incremental displacement δ was applied to the strip models uniformly along their right-edge until the strips reached a displacement δ equal to 50 mm, or a total uniform strip elongation ε_{un} ($=2\cdot\delta/L$) of 5%. During the analysis, total uniform strip elongations were noted when the maximum principal local strain ε_{max} reached values of 1, 5, 10, 15, and 20% somewhere in the strips. Isoparametric general-purpose 4-node shell element (S4) of 5 x 5 mm mesh size was used in the FE models. ASTM A572 Gr. 50 (F_y = 345 MPa) steel was selected and its behavior was represented by an idealized tri-linear stress-strain model.

Behavior of Perforated Strip Model

Fig. 2 shows strip deformations and maximum in-plane principal stress and strain contours at the surface of the shell element for the case having a 100 mm perforation diameter when ε_{max} reached a value of 20% somewhere in the strip. As shown in the figure, the in-plane principal stress and strain contours are uniform at the right edge of the strip. However, holes in the strip disturbed the “regularity” of the stress and strain flows and high stress and strain concentrations developed at the perforation edge and zones of yielding radiate out from this location at approximately 45° angles to the left and right of the perforations. In combination with Poisson’s-ratio effect, these concentrations also accounted for inward (in addition to rightward) movement of the unrestrained top edge (the interface edge to the adjacent strip) adjacent to the perforations. In an actual SPSW the interface between adjacent strips correspond to a buckle “ridge”, and this inward pull towards the hole due to Poisson’s-ratio effect would locally reduce the amplitude of the ridge.

Fig. 3a presents the effect of holes on strip global deformation where uniform distributed strip elongation ε_{un} versus perforation ratio D/S_{diag} are plotted at 1, 5, 10, 15, and 20% maximum principal local strain. At higher monitored strain ε_{max} equal to 10% to 20%, the total strip elongation decreases significantly at small perforation ratios (i.e. D/S_{diag} = 0.025 to 0.1), and then gradually increases between D/S_{diag} = 0.1 and 0.6 before slightly decreasing again for D/S_{diag} > 0.6. At the lower monitored local strain levels (i.e. ε_{max} = 1% and 5%), the total strip elongation remains almost constant for the entire range of perforation diameters.

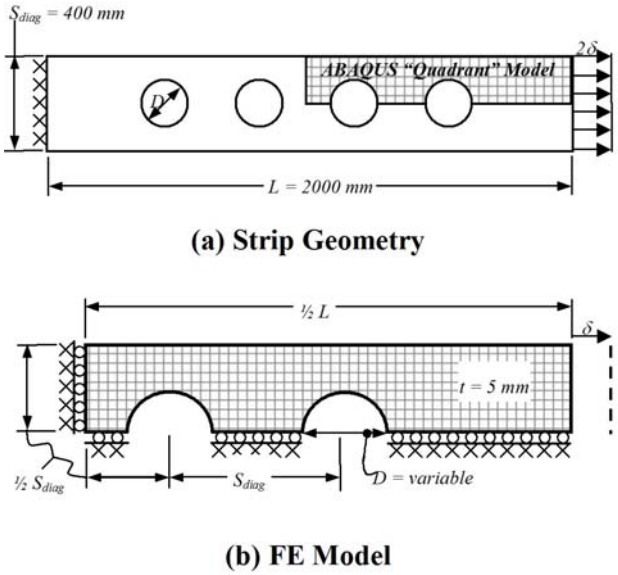

Figure 1. Individual perforated strip (Vian and Bruneau 2005)

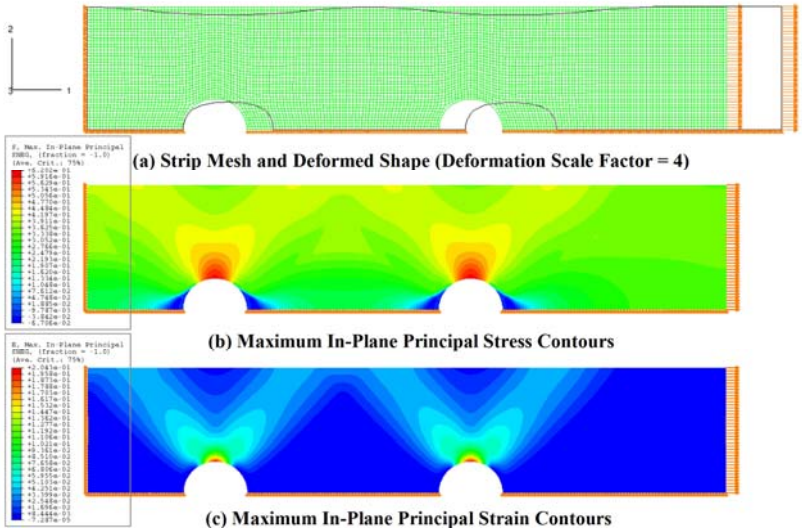

Figure 2. Typical strip analysis results at ε_{max} = 20% D = 100 mm (D/S_{diag} = 0.25)

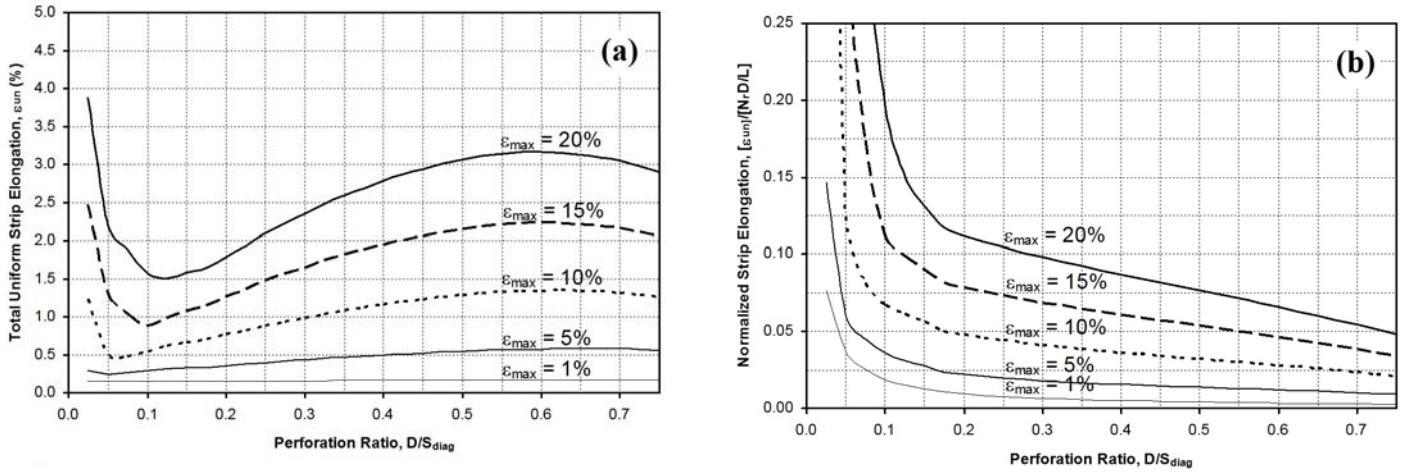

Figure 3. Strip elongation (a) real value; (b) normalized value.

To provide additional insight into this behavior, a variation of Fig. 3a is plotted in Fig. 3b by normalizing the total strip elongation by the factor $N_r.D/L$, which is the ratio of perforated length to overall length in a strip (Vian and Bruneau 2005). Simultaneously, the vertical axis is expressed as $2 \cdot \delta / N_r.D$, which is the total strip displacement divided by a total length of perforations over the entire strip. As shown in the figure, for all cases the normalized strip elongation gradually decreases as the perforation ratio increases.

Finite Element Analysis of Complete Perforated SPSW

FE models of complete perforated SPSW (panel models) were developed to verify the appropriateness and accuracy of the individual perforated strip model results and to investigate why prior results from panel analysis in Vian and Bruneau (2005) did not support the predictions from individual strip model analysis. Hence, the same specimen Vian and Bruneau (2005) previously investigated was studied for this objective.

ABAQUS/CAE, a graphical preprocessor program, was utilized to define the model of the described specimen. Omitting the "fish plate", the infill plates were connected directly to the beams and columns, the effects of this assumption to the overall behavior of SPSWs were found to be small (Driver *et al.* 1997). The meshes started with 50 x 50 mm shell elements near the boundary elements and gradually reducing to an average dimension of 35 x 35 mm per shell element adjacent to the perforations. The entire infill plate and boundary elements were meshed using the S4R shell elements, isoparametric general-purpose 4-node shell element with reduced integration and hourglass control. ASTM A572 Gr. 50 steel (F_y = 345 MPa) was selected for boundary elements and infill plate. The unidirectional idealized tri-linear stress-strain was used to model the infill plate steel while the cyclic stabilized backbone stress-strain curve comparable to the Ramberg-Osgood hysteresis was used in the boundary elements for the same steel grade.

To help initiate panel buckling and development of tension field action, an initial imperfection was applied to the models analyzed, which its magnitude was a function of the first 20 mode shapes. *CONN3D2* connector elements were used to model the hinges at the base of the Vian and Bruneau (2005) specimen in the ABAQUS model. This connector links reference nodes at the location of the hinges center, 850 mm below the centerline of bottom beam, to the corner nodes at the tip of each column flange and at the intersection of the flanges and web, and provides effectively a rigid beam connection between two nodes. At the two reference nodes, only rotation about the axis perpendicular to the plane of the wall is allowed, to replicate the hinge rotation in Vian and Bruneau test specimen. The exterior nodes of the flange elements around the perimeter of the panel zones at the top of columns were restrained against out-of-plane movement to replicate the experimental setting of Vian and Bruneau tests. A monotonic pushover displacement was applied to a reference node located at the middle centerline of the top beam. Fig. 4 shows the resulting FE model. During the analysis, frame drifts and strip elongations were measured when the maximum principal local strain ε_{max} somewhere in the infill plate reached values of 1, 5, 10, 15, and 20%.

Behavior of Perforated SPSW Considering Alternative Models

At large in-plane drifts, a first model having the boundary conditions described above experienced lateral torsional buckling, primarily at the top beam and slightly at the bottom beam (not shown here). This phenomenon also affected the columns displacement as the left column deformed in a manner not parallel to the right column. The model was then revised to have lateral supports restraining the out-of-plane movement of the boundary nodes and called the Flexible Beam Laterally Braced (FLTB) model. In addition, fine meshes were used in this model, starting with 25 x 25 mm shell elements near the boundary elements and gradually reducing to an average dimension of 15 x 15 mm per shell element adjacent to the perforations.

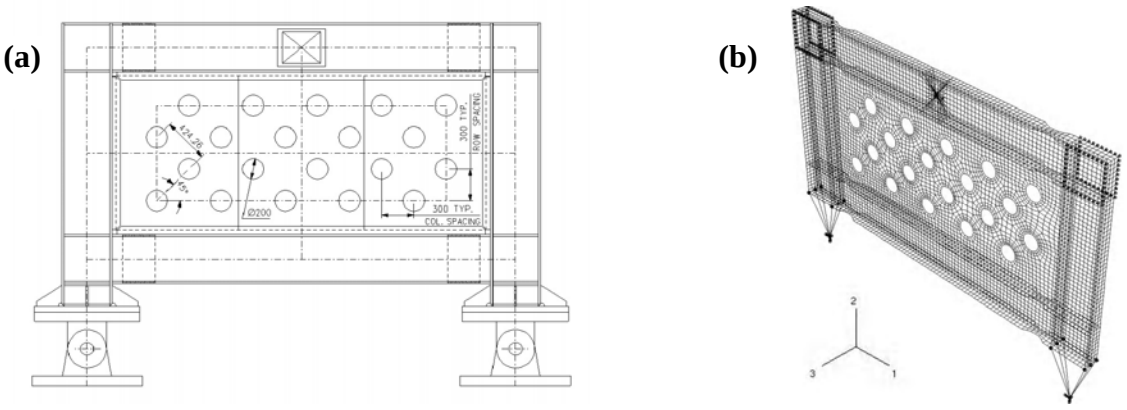

Figure 4. Perforated SPSW (a) Specimen (Vian and Bruneau 2005); (b) FE model.

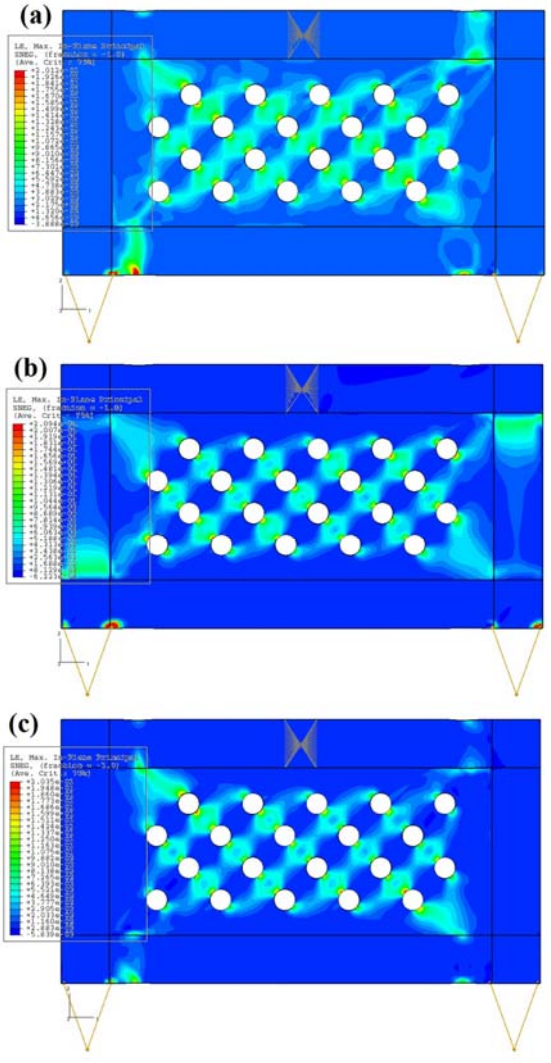

Figure 5. Typical perforated panel results at ε_{max} = 20% of (a) FLTB; (b) RF; (c) RB model.

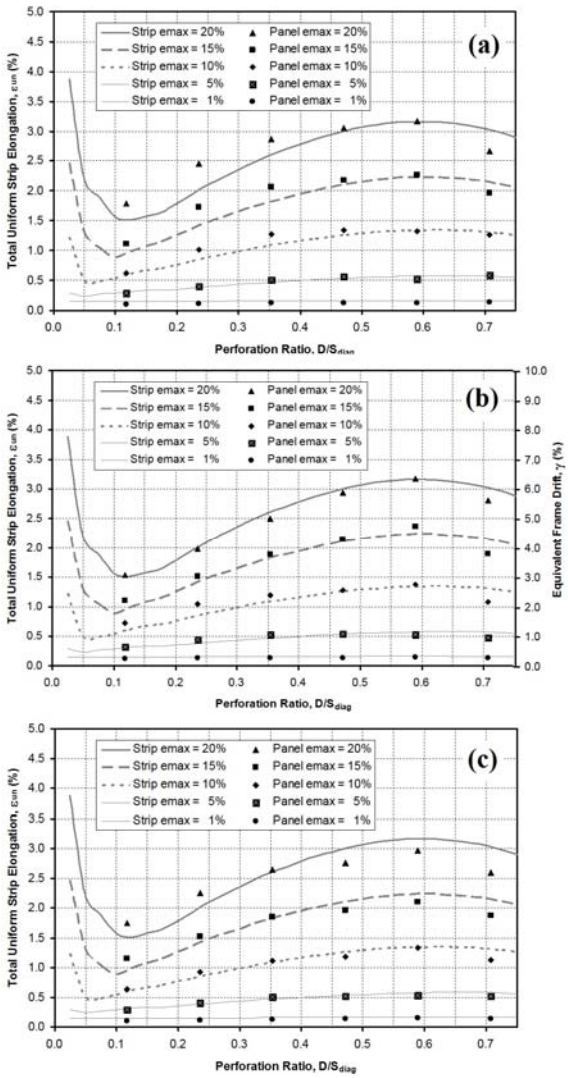

Figure 6. Uniform distributed strip axial strain ε_{un} versus perforation ration D/S_{diag} (a) FLTB; (b) RF; (c) RB model.

For the FLTB model, analysis results showed that every strip reached a different strip elongation. In particular, only one strip matched the individual strip results, while the elongation observed for the other strips in the SPSW panel was less than that for the corresponding stand-alone strip, by as much as 22% at 20% maximum principal local strain in the infill plate. The non-symmetrical beam deflections under the applied diagonal tension from the infill plate caused these deflections and resulting unequal strip axial deformations.

To investigate the significance of beam deformations on strip elongations, the FLTB model was modified by adding vertical constraints at the boundary nodes at the beams flanges (to approximate a rigid-body motion) and called the Rigid Floor (RF) model. For the RF model, the analysis results showed that all strips reached about the same elongation and matched the results obtained for the individual strip model.

Note that in the RF model, plastic hinges were constrained to occur in the columns by artificially making the beams infinitely rigid across the entire width of the SPSW. This was done as an interim measure to establish the linkages between full plate behavior and the simplified individual strips. As demonstrated, such a match exists and difference between results for actual unconstrained SPSW and individual strips are primarily due to flexibility of the top and bottom beams, and not some of the other factors (e.g. plate buckling, initial imperfections, etc). To further the understanding of how strip elongations in actual SPSW relate to the individual strip model, an alternative Rigid Beam (RB) model was considered. In this model, a very stiff beam between the RBS is modeled by increasing the thickness of the flanges and webs to be 10 times thicker than for the actual beam. The RBS segments remained at their actual thickness and unconstrained. This allows the rigid-body motions of the beams (translations and rotations) and development of plastic hinges at the RBS connections (as would be expected in correctly designed SPSW).

For the RB model, the ‘full’ strips elongated by almost the same amount varying from 2.35% to 2.75% at 20% maximum principal local strain. This could be attributed to the “kink” that occurred at the RBS connections that are the reference points from which the two outer strips axial deformations are measured. At lower monitored strain (i.e., ε_{max} = 5%), however, the difference was significantly less since the RBS connections were not severely yielded. Nevertheless, the middle strips elongations were 8% and 11% lower than those of their corresponding individual strip, respectively, at the monitored strain $\varepsilon_{max} \geq 10\%$, which “corner effect” may contribute to this discrepancy. Here, results of the RB model are considered acceptable for all practical purposes.

Fig. 5 presents the in-plane principal maximum strain contours of the three models considered. The distribution of tension field action around the perforations is similar to that observed by Vian and Bruneau (2005). During pushover analysis, yielding was observed to initiate with concentrations at the perforation edges, with zones of yielding radiating out from this location at approximately 45° angles with respect to the diagonal tension field orientation, and then overlapping with yielding zones of adjacent holes from different strips, before finally flowing into the RBS connections (FLTB and RB model) or into the columns (RF model).

Effects of Perforation Ratios and Number of Perforations

To examine the effect of perforation ratios and number of perforations, a series of SPSW using the three analyzed models with perforation diameter D = 50, 100, 150, 200, 250, and 300 mm was developed and analyzed. This data set allows observation of the trends in SPSW behavior compared to the individual strip results plotted in Fig. 6.

Fig. 6 shows the results for the FLTB, RF, and RB models, respectively. In the FLTB model, some differences between the SPSW panel strips and the individual strips results are observed at 15 and 20% monitored strain for smaller perforation diameters. For example at 20% monitored strain and 100 mm perforation diameter, the differences between the two are as much as 23%. The RF model having perforated panel with the 200 mm diameter holes matched well the individual strip model results. Some insignificant differences occurred at the smaller perforation ratio D/S_{diag} = 0.118 and 0.236 at the 5 and 10% monitored strain levels. Moreover in the RB model, though some differences between the SPSW panel strips and the individual strip results are observed at the 20% monitored strain, at lower monitored strain however the two models are in a good agreement. A less than 15% difference was observed and considered acceptable.

Panel Strength Design Equation

It had earlier been proposed (Roberts and Sabouri-Ghomi 1992) that the strength of a perforated panel $V_{yp.perf}$ could be conservatively approximated by applying a linear reduction factor to the strength of a solid panel V_{yp}, with same overall dimensions. The proposed reduction was developed from a single holed panel. Results of analyses performed with the panel SPSW model were used to re-assess the applicability of that relation for SPSW panels having multiple perforations taking into account the refinements in analysis considered in this study. For comparison purposes, a SPSW having a solid infill panel was also analyzed. This model had the same characteristics as the one used to analyze perforated panels. For both the solid and perforated SPSW models, the infill panel strength was determined by subtracting the strength of the bare frame (determined from an additional analysis of the boundary frame alone) from the total SPSW strength. Results and discussion are only presented for the RF and RB model.

Fig. 7 presents infill plate strength ratios ($V_{yp.perf}/V_{yp}$) versus perforation ratios (D/S_{diag}) for frame drifts (γ) of 1, 2, 3, 4 and 5%. Additionally, the predicted value is also plotted in this figure (as a solid line). For simplicity, linear regression was applied on a new proposed equation as follows:

$$V_{yp.perf} = \left[1 - \alpha \frac{D}{S_{diag}}\right] \cdot V_{yp} \tag{1}$$

where α is a proposed regression factor equal to 0.70. In Fig. 7, the results of a linear regression analysis performed on the FE data is plotted as a dotted line. This equation matches within 5% on average the actual data series. This proposed equation is only valid for a wall with a regular grid of uniformly distributed holes covering the entire plate surfaces, as shown in Fig. 7. The equation has been validated for geometries D/S = 0.12 to 0.71. For example, a wall having a single hole cannot be used using the proposed equation.

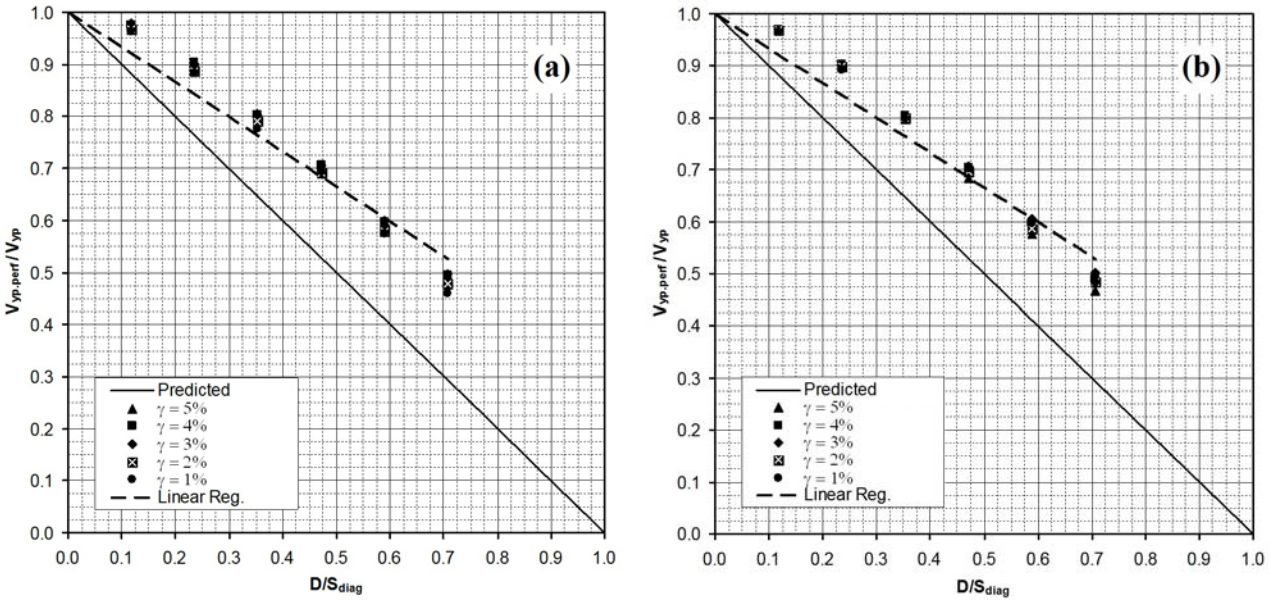

Figure 7. Infill plate strength ratios versus perforation ratio (a) RF; (b) RB model

Design Recommendations and Considerations

Design recommendations for unstiffened thin SPSW having openings are suggested below.

1. The behavior of individual strips can accurately predict the behavior of complete perforated SPSW provided the holes diameter is less than 60% of the strip width. On that basis, if performance of complete SPSW systems with the aforementioned perforation layout is to be evaluated using simpler models, the perforation ratio of SPSW should be limited to $D/S_{diag} \leq 0.6$, which is a range that should accommodate most practical needs.
2. No interaction exists between adjacent strips that could affect the stress distribution within an individual strip, i.e., each strip in a SPSW behaves as an independent strip.
3. The shear strength of perforated infill plate for SPSW having multiple circular perforations regularly spaced throughout the infill can be calculated by reducing the shear strength of the plate in a solid panel SPSW by a factor $(1-\alpha \cdot D/S_{diag})$, where α is a proposed correction factor equal to 0.70. For panel strength calculated on that basis, the full shear strength of the complete SPSW is conservatively obtained by adding to this value the strength of the boundary frame without the infill.

These design recommendations capture the behavior observed experimentally, and it is recognized that they are limited to the type of regular perforation layout considered here. Future research may allow to investigate other perforation layouts, while providing additional opportunities to validate the proposed design equations.

Conclusions

Finite element monotonic pushover analysis was performed to investigate the behavior of unstiffened thin SPSW having a regular pattern of openings. Individual perforated strips were first analyzed to develop a fundamental understanding of the behavior of complete perforated

SPSW. A series of one-story SPSW having multiple perforations on panels was then considered, with variation in perforation diameter and boundary conditions. The objective of this analysis was to verify the accuracy of results obtained from finite element analysis of individual perforated strips to predict the strength of complete SPSW by summing the strength of "simpler" individual strips. Good agreement in overall behavior between the three models considered and the individual perforated strip model was observed. These models were used to formulate the design recommendations presented in the previous section.

Acknowledgements

Analytical work in this study was performed at the Center for Computational Research at the University at Buffalo, the State University of New York. This work was supported by the Earthquake Engineering Research Centers Program of the National Science Foundation under award number ECC-9701471 to the Multidisciplinary Center for Earthquake Engineering Research. However, any opinions, findings, conclusions, and recommendations presented in this paper are those of the authors and do not necessarily reflect the views of the sponsors.

References

Behbahanifard, M. R., Grondin, G. Y., and Elwi, A. E. (2003). "Experimental and Numerical Investigation of Steel Plate Shear Wall." *Structural Engineering Report 254*, Department of Civil Engineering, University of Alberta, Edmonton, Alberta, Canada.

Berman, J. W. and Bruneau, M. (2005). "Experimental Investigation of Light-Gauge Steel Plate Shear Walls." *Journal of Structural Engineering*, ASCE, Vol. 131, No. 2, pp. 259-267.

Driver, R. G., Kulak, G. L., Kennedy, D. J. L., and Elwi, A. E. (1997). "Seismic Behavior of Steel Plate Shear Walls." *Structural Engineering Report 215*, Department of Civil Engineering, University of Alberta, Edmonton, Alberta, Canada.

Purba, R., and Bruneau, M. (2007). "Design Recommendations for Perforated Steel Plate Shear Walls" *Technical Report* MCEER-07-0011, Multidisciplinary Center for Earthquake Engineering Research, State University of New York at Buffalo, Buffalo, New York.

Roberts, T. and Sabouri-Ghomi, S. (1992). "Hysteretic characteristics of unstiffened perforated steel plate shear panels." *Thin Walled Structures*, Vol. 14, pp. 139-151.

Sabelli, R. and Bruneau, M. (2007). "Steel Plate Shear Walls (AISC Design Guide)", American Institute of Steel Construction, Inc., Chicago, Illinois, 144 p.

Thorburn, L. Jane, Kulak, G. L., and Montgomery, C. J. (1983). "Analysis of Steel Plate Shear Walls." *Structural Engineering Report No. 107*, Department of Civil Engineering, University of Alberta, Edmonton, Alberta, Canada.

Timler, P. A. and Kulak, G. L. (1983). "Experimental Study of Steel Plate Shear Walls." *Structural Engineering Report No. 114*, Department of Civil Engineering, University of Alberta, Edmonton, Alberta, Canada.

Vian, D., and Bruneau, M. (2005). "Steel plate shear walls for seismic design and retrofit of building structures." *Tech. Rep. MCEER-05-0010*, Multidisciplinary Center for Earthquake Engineering Research, State University of New York at Buffalo, Buffalo, New York.